

See discussions, stats, and author profiles for this publication at: <https://www.researchgate.net/publication/6507346>

Mimicking Early Events of Virus Infection: Capillary Electrophoretic Analysis of Virus Attachment to Receptor-Decorated Liposomes

ARTICLE *in* ANALYTICAL CHEMISTRY · MARCH 2007

Impact Factor: 5.64 · DOI: 10.1021/ac061728m · Source: PubMed

CITATIONS

18

READS

10

5 AUTHORS, INCLUDING:



Jürgen Wruss

Fachhochschule Oberösterreich

10 PUBLICATIONS 333 CITATIONS

SEE PROFILE



Dieter Blaas

Medical University of Vienna

186 PUBLICATIONS 6,409 CITATIONS

SEE PROFILE



Ernst Kenndler

University of Vienna

258 PUBLICATIONS 6,364 CITATIONS

SEE PROFILE

Mimicking Early Events of Virus Infection: Capillary Electrophoretic Analysis of Virus Attachment to Receptor-Decorated Liposomes

Gerhard Bilek,^{†,‡} Leopold Kremser,[†] Jürgen Wruss,[‡] Dieter Blaas,[‡] and Ernst Kenndler^{*,†}

Institute for Analytical Chemistry, University of Vienna, A-1090 Vienna, Austria, and Max F. Perutz Laboratories, Vienna Biocenter, Medical University of Vienna, Vienna, Austria

The attachment of human rhinovirus serotype 2 to an artificial cell membrane was followed by capillary electrophoresis. The cell membrane was mimicked by liposomes (average diameter of about 190 nm) containing a lipid with a nitrilotriacetic acid (NTA) group. This group, in the presence of Ni^{2+} ions, served as anchor for the his_6 -tags of recombinant derivatives of the very-low-density lipoprotein (VLDL) receptor comprising either modules 1, 2, and 3 (V123) or five tandem copies of module 3 (V33333). We demonstrate by capillary electrophoresis with laser induced fluorescence detection of the liposomes that the minor receptor group rhinovirus HRV2 binds specifically to the receptor-decorated vesicles; the major receptor group rhinovirus HRV14, which uses a different receptor for cell binding, does not attach to the liposomes.

The very first event in virus infection is the specific attachment of the virion to structures at the host cell membrane, which are termed “virus receptors”, neglecting the fact that their original function lies in cell–cell interaction and/or metabolism of the cell. Viruses have adapted to exploit these molecules for their proper benefit. The membrane of eukaryotic cells is complex and contains many different proteins attached to or embedded in the lipid bilayer. This complicates the analysis of virus binding to specific receptors in their biological context. A simpler system, mimicking the cell membrane with its physicochemical properties but containing only one type of protein at the time, can be realized with liposomes. These vesicles can be made to carry the proteins of choice attached by various means like insertion via hydrophobic transmembrane sequences, binding via covalently linked lipids, or by making use of noncovalent attachment of the proteins to suitable functional groups connected to chemically modified lipids. Based on the latter concept, in the present work, we established a model for the interaction between a minor group human rhinovirus (HRV) and its cognate receptors, members of the low-density lipoprotein receptor family, and used capillary electrophoresis (CE) for its analysis.

Modeling of virus attachment was carried out in different steps, as depicted schematically in Figure 1. First, liposomes were

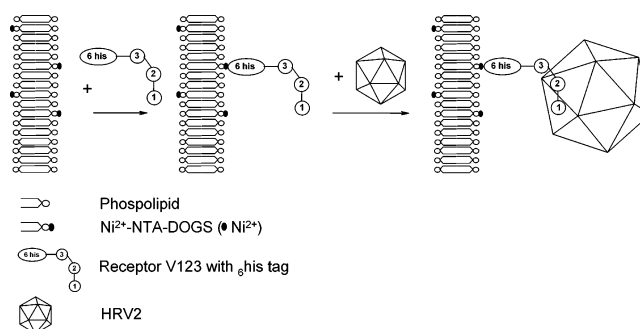


Figure 1. Schematic representation of the attachment of HRV2 to the liposome membrane. A ternary adduct is formed from the Ni^{2+} –NTA–implanted liposome, receptor construct V123, and HRV2. A part of the liposome bilayer is shown that contains the NTA–lipid with complexed Ni^{2+} ions. The receptor construct binds via its his_6 -tag to the membrane surface by complexation with the Ni^{2+} ions. Finally, HRV2 binds biospecifically to the liposome surface via the modules of the receptor construct. The average diameter of the liposomal vesicles is about 190 nm, their bilayer thickness is about 5 nm, and HRV2 diameter is about 30 nm. Note that the MBP fused to the N-terminus of the receptor is depicted.

prepared from standard lipids including nitrilotriacetate (NTA)-modified dioleoyl-glycerol complexed with Ni^{2+} -ions. A recombinant soluble receptor construct containing a hexa-histidine tag (his_6 -tag) at its C-terminus was then attached via the Ni^{2+} –NTA–lipid to the liposome surface. As a result, a receptor-decorated vesicle was formed modeling the cell membrane. Finally, virus was attached to these receptor-decorated vesicles via biospecific interaction. All individual steps were followed by CE via laser-induced fluorescence (LIF) detection of a fluorescent dye dissolved in the aqueous vesicle core of the liposomes.

EXPERIMENTAL SECTION

Instrumentation. CE with LIF detection was carried out with a homemade instrument consisting of an Ar-laser (Reliant 50S-489, 50 mW, Laser-Physics), a high voltage power supply unit (HNC 20.000, Heinzinger Electronic, Germany), and an optical bench where the fluorescence light was focused by a microscopic lens system and passed through a cutoff filter (500 nm) before reaching the photomultiplier (Hamamatsu H5785, Shimokanzo, Japan). Data were collected with the DataApex software (Prague, Czech Republic). A PVA-coated capillary (30.0/21.5 cm length, 75 or 100 μm inner diameter (ID); Agilent, Waldbronn, Germany) was used with the detection window placed at the anodic side of

* To whom correspondence should be addressed. E-mail: ernst.kenndler@univie.ac.at.

[†] University of Vienna.

[‡] Medical University of Vienna.

the instrument. The capillary was positioned in still air at room temperature ($\sim 25^\circ\text{C}$) without thermostating. The background electrolyte for the CE analysis of the liposomes consisted of tris-(hydroxymethyl)-aminomethan (Tris)/HCl (50 mmol L^{-1} , pH 8.0). Experiments were performed at a constant voltage of -5 kV ; the resulting current was about $21\text{ }\mu\text{A}$. Samples were applied by hydrodynamic injection at the cathodic side of the capillary by lifting the sample vial by 3 cm for 12 s .

CE with UV detection was performed with an automated HP3D instrument (Agilent) equipped with a diode array UV-vis detector ($190\text{--}600\text{ nm}$). An untreated fused-silica capillary ($68.0/59.5\text{ cm}$ length, $75\text{ }\mu\text{m}$ ID; Composite Metal Services Ltd.) was used and thermostated at 20°C . The separation buffer was prepared by adjusting boric acid (100 mmol L^{-1}) with NaOH to pH 8.3 and adding SDS to 10 mmol L^{-1} . The applied voltage was $+20\text{ kV}$, with the UV detector placed at the cathodic side of the capillary; the resulting current was about $25\text{ }\mu\text{A}$. Samples were injected by 25 mbar pressure for 10 s .

The average vesicle diameter and the size-distribution of purified liposome preparations were determined by using dynamic light scattering on a Zetasizer (Malvern Nano-ZS, Malvern instruments, U.K.). The suspensions of the liposomes were diluted with 50 mM Tris-HCl (pH 8.0) to a concentration appropriate for the measuring range of the instrument. This is described in more detail in ref 1.

The Ni concentration of the liposomes was determined by atomic absorbance spectroscopy (AAS) using a 4100 ZL instrument (Perkin-Elmer) with a transverse heated graphite atomizer in the stabilized temperature platform furnace technique and Zeeman-effect background correction (longitudinal). A Ni hollow cathode lamp (25 mA , slit 0.2 mm , wavelength: 232.0 nm) was used. Sample volume was $20\text{ }\mu\text{L}$; analyses were performed without chemical modifiers. The organic matrix was dry ashed in the graphite tube with air at 500°C . For the individual steps of analysis, the following temperatures were applied: ashing, 500°C , pyrolysis, 1100°C , atomization, 2400°C , cleaning, 2450°C . Ar flow was 250 mL min^{-1} .

Reagents. Liposomes were made from 1-palmitoyl-2-oleoyl-*sn*-glycero-3-phosphocholine (POPC), 1- α -phosphatidylethanolamine (PE), cholesterol (Ch), the ammonium salt of 1,2-distearoyl-*sn*-glycero-3-phosphoethanolamine-*N*-[methoxy(polyethyleneglycol)-750] (DSPE-PEG), and the Ni^{2+} salt of 1,2-dioleoyl-*sn*-glycero-3-[(*N*-(5-amino-1-carboxypentyl) iminodiacetic acid) succinyl] (Ni^{2+} -NTA-DOGS), all obtained from Avanti Polar Lipids (Alabaster, AL, distributor Instruchemie B.V., Netherlands). HCl, NaOH, boric acid, and chloroform (p.a.) were from E. Merck (Darmstadt, Germany). Tris and fluorescein isothiocyanate (FITC)-dextran (70 kDa) were from Sigma (Milwaukee, WI). Fluorescence latex beads used as standards in size exclusion chromatography (SEC) were from Polysciences (Warrington, PA).

The major group rhinovirus HRV14 and the minor group rhinovirus HRV2 were grown in HeLa H1 suspension culture and purified as described elsewhere.² The virus concentration and the purity of the virus were monitored by CE.³ The virus stock solutions were at 5.7 mg/mL (HRV2) and 1.3 mg/mL (HRV14).

Two recombinant soluble receptor constructs, derived from the human very low-density lipoprotein receptor (VLDLR), were expressed and purified as described.⁴ Both were expressed and used for all experiments as fusion proteins, carrying at their N-terminus the maltose-binding protein (MBP) and at their C-terminus a his₆-tag. V123 comprises the first three ligand binding modules of VLDLR, and V33333 is an artificial concatemer of five copies of the third module of VLDLR. They exhibit different functional affinity (avidity) toward HRV2.^{5,6} The concentration of the respective receptor stock solutions was 8 mg/mL for V123 and 2 mg/mL for V33333.

SEC was carried out on a Sephacryl S-1000 column from GE Healthcare, Uppsala, Sweden.

Procedures. Multilamellar vesicle (MLV) suspensions were prepared by dissolving POPC, PE, Ch, DSPE-PEG, and Ni^{2+} -NTA-DOGS in chloroform to produce separate lipid stocks with a concentration of 10 mg/mL each. These chloroform stocks were combined in a 50 mL pointed flask at a ratio of POPC:PE:Ch:DSPE-PEG: Ni^{2+} -NTA-DOGS = $26:24:40:5:5$ [mol %] to produce Ni^{2+} -NTA implanted vesicles with PEG grafting as described in ref 1. Briefly, the organic solvent of the final mixture (approximately 1.5 mL) was removed under vacuum by the aid of a rotary evaporator. To ensure uniform deposition of the lipids as a thin film, the bottom settings were redissolved twice in 1.5 mL of chloroform followed by immediate evaporation. The last evaporation was conducted for at least 4 h to ensure complete removal of traces of the solvent. Subsequently, the lipid film was hydrated in 2.5 mL of 50 mmol L^{-1} Tris-HCl (pH 8.0), containing $70\text{ }\mu\text{mol L}^{-1}$ FITC-dextran to label the vesicles. After $30\text{--}60\text{ min}$ at 65°C in a water bath, MLVs were produced by $3\text{--}6$ freeze/thaw cycles; the lipid suspension was frozen in liquid nitrogen, thawed at 65°C in a water bath, and vortexed to peel off the lipid film. To avoid oxidation, freshly produced MLVs were gassed with N_2 before storing them at -20°C in the dark.

To form large unilamellar vesicles (LUVs) that better mimic the cell surface, MLVs were passed through two polycarbonate filters with a pore diameter of 400 nm by the aid of an extruder (Mini-Extruder, Avanti Polar Lipids) at 65°C to prevent aggregation of the rigid lipid membranes. Under this condition, all lipids are above their phase transition temperature and in a liquid-crystal state. The suspension was passed 21 times through the filters. The resulting LUVs were stored under N_2 atmosphere at 4°C in the dark.

Vesicles were separated from free FITC-dextran and other low-molecular weight contaminants by SEC, using a Sephacryl S-1000 column ($30\text{ cm} \times 1\text{ cm}$). The column was equilibrated with 50 mM Tris-HCl (pH 8.0), and its void volume was determined at $250\text{ }\mu\text{L/min}$ with fluorescent latex beads (200 nm diameter; $120\text{ }\mu\text{L}$ of a $1:100$ dilution of the stock). Next, the LUV suspension ($120\text{ }\mu\text{L}$) was applied, and SEC was carried out with the same mobile phase at the same flow rate; fractions of $300\text{ }\mu\text{L}$ were collected. The liposomes eluted with the void volume as deter-

(1) Bilek, G.; Kremser, L.; Blaas, D.; Kenndler, E. *Electrophoresis* **2006**, *27*, 3999–4007.

(2) Kienberger, F.; Zhu, R.; Moser, R.; Blaas, D.; Hinterdorfer, P. *J. Virol.* **2004**, *78*, 3203–3209.

(3) Okun, V. M.; Ronacher, B.; Blaas, D.; Kenndler, E. *Anal. Chem.* **1999**, *71*, 2028–2032.

(4) Ronacher, B.; Marlovits, T. C.; Moser, R.; Blaas, D. *Virology* **2000**, *278*, 541–550.

(5) Moser, R.; Snyers, L.; Wruss, J.; Angulo, J.; Peters, H.; Peters, T.; Blaas, D. *Virology* **2005**, *338*, 259–269.

(6) Okun, V. M.; Moser, R.; Ronacher, B.; Kenndler, E.; Blaas, D. *J. Biol. Chem.* **2001**, *276*, 1057–1062.

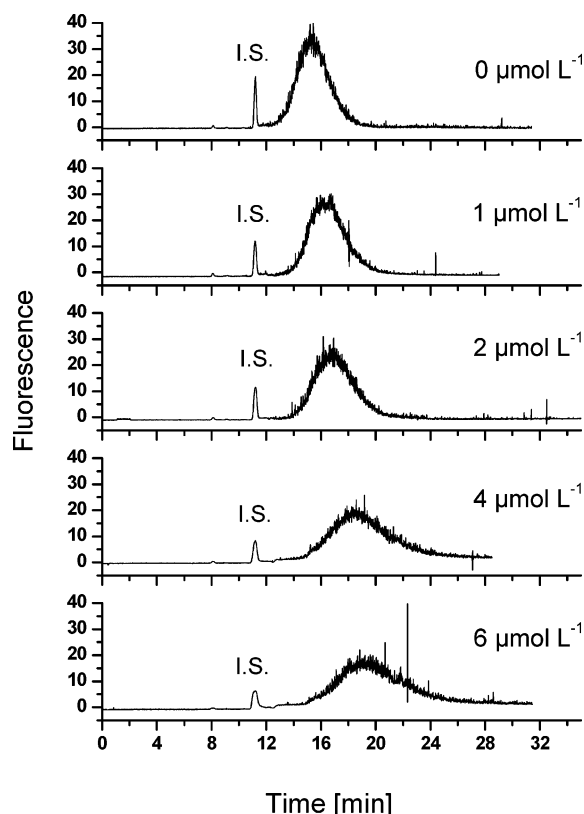


Figure 2. Electropherograms of liposomes containing Ni^{2+} -NTA-carrying lipid, incubated with increasing concentration of V33333 (between 1 and $6 \mu\text{mol L}^{-1}$). Liposome composition: POPC:PE:Ch:DSPE-PEG: Ni^{2+} -NTA-DOGS = 26:24:40:5:5 mol %, FL-labeled with FITC-dextran ($70 \mu\text{mol L}^{-1}$). Ni^{2+} -NTA concentration (5% of total lipid) accessible for receptor binding in the incubation mixture is $1.8 \mu\text{mol L}^{-1}$. I.S. internal standard (fluorescein), 2 nmol L^{-1} . CE-conditions: PVA capillary, 30 cm/21.5 cm length, ID $75 \mu\text{m}$. BGE: Tris-HCl, 50 mM, pH 8.0. Voltage, -5 kV ; current, $21 \mu\text{A}$. Hydrodynamic injection at the cathodic side (lifting the inlet by 3 cm for 12 s). Temperature 25°C ; fluorescence detection at 488 nm excitation wavelength and 500 nm cutoff.

mined by fluorimetry, using a 96-well plate reader (Wallac 1420 VICTOR V, Perkin-Elmer, Finland) set at 485 nm excitation and 535 nm emission wavelength. Fractions were also subjected to UV spectrometry at 280 nm (Hitachi U-2000 spectrophotometer) to confirm the location of the peak.

RESULTS AND DISCUSSION

Receptor-Decorated Liposomes. VLDL-receptors are mosaic proteins that most probably evolved from single modules and building blocks. Their ligand-binding domains at the N-terminus are composed of various numbers of ligand binding repeats or type A modules, each about 40 amino acids in length, among them 6 cysteines that are all engaged in disulfide bridges. VLDLR has 8 ligand binding repeats. V33333 is a synthetic soluble receptor construct; it is a concatemer of five copies of module 3 of VLDLR fused to MBP. The complete receptor construct (including MBP) consists of 620 amino acids and has a molecular mass of 67 439 Da. As it possesses a 6 histidine tag, it binds to Ni^{2+} -NTA of the NTA-DOGS lipid present in the liposome membrane. The resulting vesicles can be considered a simplified model of a cell with epitopes for viral attachment. For decoration with the receptor

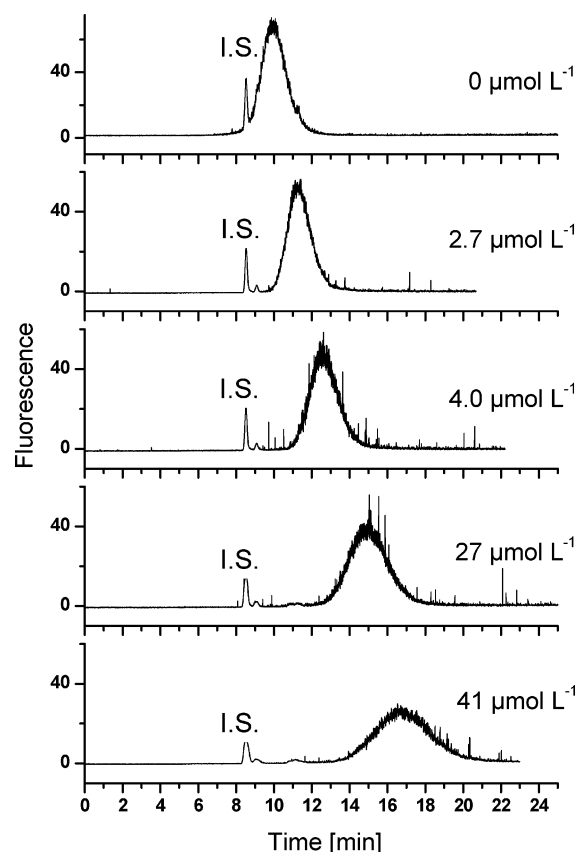


Figure 3. Electropherograms of Ni^{2+} -NTA-lipid containing liposomes after incubation with increasing concentrations of V123 (between 2.7 and $41 \mu\text{mol L}^{-1}$). Ni^{2+} -NTA concentration (5% of total lipid) accessible for receptor binding in the incubation mixture is $2.0 \mu\text{mol L}^{-1}$. Liposome composition and CE conditions are as in Figure 2.

constructs, the Ni^{2+} -NTA-implanted liposomes were reacted with V33333 with increasing concentrations (between 1 and $6 \mu\text{mol L}^{-1}$), and the resulting products were analyzed by CE-LIF. The electropherograms are shown in Figure 2. It can be seen that a typical, relatively broad liposome peak is obtained, which gradually shifts to longer migration time with increasing V33333 concentration in the reaction mixture. The change in the mobility clearly demonstrates attachment of the receptors to the liposome surface; the broadening of the peak with increasing receptor concentration is most probably due to heterogeneity resulting from a mixture of liposomes carrying different numbers of receptors.

Similarly, another recombinant soluble receptor construct, V123, was attached to the functionalized liposomes. This fragment consists of the first three modules of VLDLR. V123 encompasses 535 amino acid residues with a total molecular mass of 59122 Da. As V33333, V123 is fused to MBP and carries a C-terminal his₆-tag. The electropherograms obtained upon incubation of the Ni^{2+} -NTA-functionalized liposomes at increasing concentrations of V123 are depicted in Figure 3. The liposome suspension had approximately the same concentration as in the experiments described for V33333. Again, upon addition of increasing amounts of V123 (from 2.7 to $68 \mu\text{mol L}^{-1}$), a gradual shift of the liposome peak was observed. The plateau of its mobility at the higher concentrations of the receptor in the incubation mixture (Figure 4) indicates that saturation with the receptor occurs above $\sim 35 \mu\text{mol L}^{-1}$. Saturation was not attained with V33333, as the

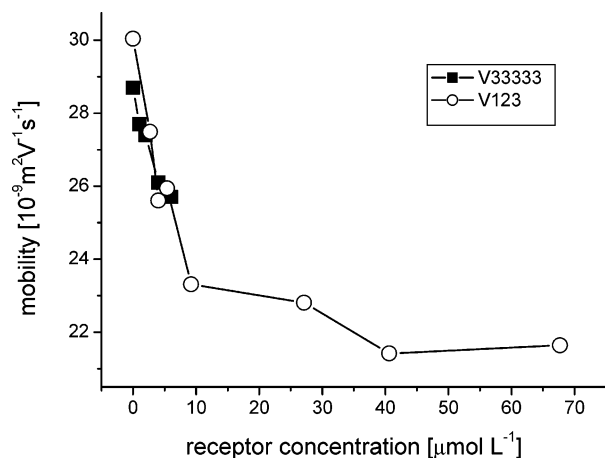


Figure 4. Mobilities of the liposomes (as measured at the apex of the peaks shown in Figures 2 and 3) at different concentrations of the recombinant receptor fragments V123 and V33333, respectively, in the incubation mixture with the Ni²⁺–NTA-carrying vesicles. The mobilities were typically reproducible within $1 \times 10^{-9} \text{ m}^2 \text{ V}^{-1} \text{ s}^{-1}$, according to a relative standard deviation of about 4% (for 3–5 measurements).

concentration of the available stock solution was lower than that of V123 (see Experimental Section).

The Ni²⁺-concentration in the samples was determined by AAS (note that the Ni–NTA-containing lipid contributed only 5% of total lipid). The Ni²⁺ concentration as obtained after size exclusion chromatography of the liposomes was estimated to about $16 \mu\text{mol L}^{-1}$. Consequently to dilution upon addition of V33333, the final Ni²⁺ concentration was thus $3.6 \mu\text{mol L}^{-1}$. Because one-half of the NTA is located at the inner face of the liposome and is thus not accessible, roughly $1.8 \mu\text{mol L}^{-1}$ of the Ni²⁺–NTA is available for complex formation with the his₆-tagged receptor (for concentrations of the components in the other binding experiments, see figure legends). It is remarkable that the receptor concentration required to reach the plateau of the binding curve is considerably higher. Several causes can be responsible for this effect. The most probable reason is the dissociation of the Ni²⁺–NTA/receptor complex; the equilibrium dissociation constant of the binding reaction between Ni²⁺–NTA and a his₆ tag is about 10^{-5} – $10^{-6} \text{ mol L}^{-1}$.^{7–9} As this is within the concentration range of the analytes in the incubation mixture, an excess of receptor fragment is needed to shift the equilibrium toward the complex.

Virus Attachment to Receptor-Decorated Liposomes.

When free in solution, V33333 binds to HRV2, as demonstrated by using CE in our previous papers.^{10,11} We determined the composition of the V33333–HRV2 complex at saturation with 12 receptors per virion. However, interaction of the virus with the cell surface does not involve soluble receptors but rather receptors that are firmly anchored within the membrane. In the present

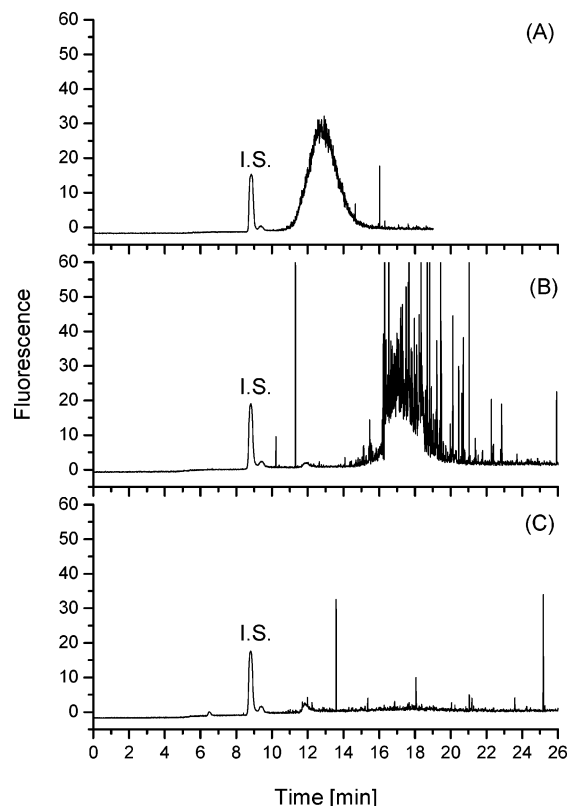


Figure 5. Electropherograms of (A) liposomes decorated with V33333, (B) liposomes as in (A), incubated with HRV2, and (C) liposomes carrying HRV2 as in (B), after 40 min sonication. Liposome composition and CE conditions are as in Figure 2. Incubation condition (in $100 \mu\text{L}$): (A) Ni²⁺–NTA:V33333 = 1.6:7.4 ($\mu\text{mol L}^{-1}$); (B) and (C) Ni²⁺–NTA:V33333:HRV2 = 1.6:7.4:0.059 ($\mu\text{mol L}^{-1}$).

paper, we investigated the interaction of rhinoviruses with receptor fragments present on the liposome surface. This allows free diffusion within the plane of the lipid bilayer and thus mimics much better in vivo conditions than, for example, surface plasmon resonance methodology or any other assay in which one of the components, receptor or virus, is firmly attached to a solid support. Therefore, several membrane-attached receptors might be recruited by an individual virion.

Incubation of the virus with the V33333-decorated liposome results in electropherograms exhibiting a change of the vesicle peak (Figure 5). Both migration time and shape of the liposome signal were completely changed. The vesicles emerged considerably later, and the peaks were partly covered with a large number of spikes (compare Figure 5A with B). The spikes suggest that clusters of vesicles are formed with virions bridging two or more liposomes. As previously observed for plain liposomes,¹ the peak together with the spikes completely disappeared upon sonication (Figure 5C), indicating that the vesicles had been destroyed.

As for V33333, upon incubation of V123-decorated vesicles for 30 min with HRV2, the liposomal peak disappeared and a large number of spikes emerged within the region of the expected position of the vesicles carrying virus (Figure 6B). This provides evidence that complexes had indeed been formed (compare to the vesicles with attached V33333 carrying virus, Figure 5B). Additional evidence for the presence of liposome-bound virus comes from the following experiment; a sample of the putative virus-carrying vesicle was incubated with 20 mM EDTA for several

- (7) Khan, F.; He, M.; Taussig, M. J. *Anal. Chem.* **2006**, *78*, 3072–3079.
- (8) Nieba, L.; Nieba-Axmann, S. E.; Persson, A.; Hamalainen, M.; Edebratt, F.; Hansson, A.; Lidholm, J.; Magnusson, K.; Karlsson, A. F.; Pluckthun, A. *Anal. Biochem.* **1997**, *252*, 217–228.
- (9) Lata, S.; Reichel, A.; Brock, R.; Tampe, R.; Piehler, J. *J. Am. Chem. Soc.* **2005**, *127*, 10205–10215.
- (10) Nicodemou, A.; Petsch, M.; Konecni, T.; Kremser, L.; Kenndler, E.; Casasnovas, J.; Blaas, D. *FEBS Lett.* **2005**, *579*, 5507–5511.
- (11) Konecni, T.; Kremser, L.; Snyers, L.; Rankl, C.; Kilar, F.; Kenndler, E.; Blaas, D. *FEBS Lett.* **2004**, *568*, 99–104.

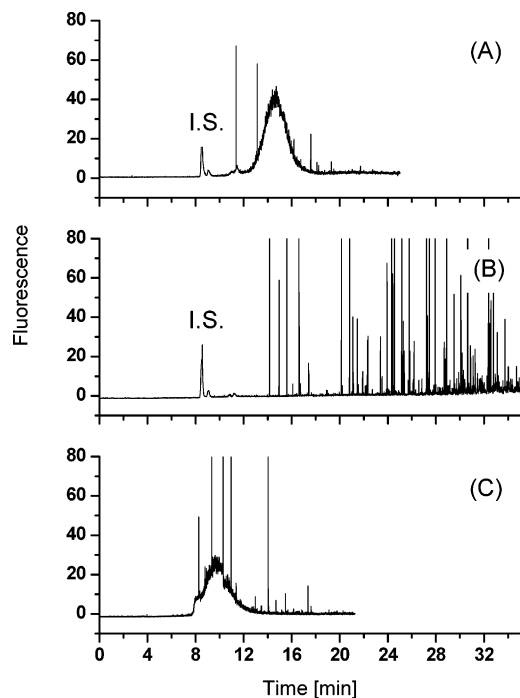


Figure 6. Electropherograms of (A) V123-decorated liposomes: Ni^{2+} -NTA-implanted liposomes incubated with V123; (B) V123-decorated liposomes as in (A), incubated with HRV2; (C) HRV2 was bound to V123-decorated liposomes as in (B), and then EDTA was added. Liposome composition and CE conditions are as in Figure 2. Incubation conditions (total incubation volume: 50 μL): (A) Ni^{2+} -NTA:V33333 = 2.0:13.5 ($\mu\text{mol L}^{-1}$); (B) Ni^{2+} -NTA:V33333:HRV2 = 2.0:13.5:0.053 ($\mu\text{mol L}^{-1}$).

minutes to destroy the Ni^{2+} -NTA complex (the binding constant of the Ni^{2+} -EDTA complex is about 7 orders of magnitude larger than that of the Ni^{2+} -NTA complex) and thus to displace the receptor from the liposome surface. As expected, the signal corresponding to bare liposome was re-established after treatment of the vesicles with EDTA (Figure 6C), thus confirming that the spikes indeed correspond to aggregates of liposomes bridged by receptor-bound virions. The signal of the recovered liposomes was slightly reduced as compared to that of the original sample because of dilution.

Taken together, our data indicate that virus becomes attached to the vesicles via the biospecific reaction with the receptor fragment. Nevertheless, more experiments were carried out to exclude any unspecific interactions. For this purpose, we investigated, by CE, whether the liposome peak changed upon addition of virus to vesicles not carrying receptor. As a further control, binding of a major group virus to receptor-decorated liposomes was assessed. As major group viruses use intercellular adhesion molecule 1, ICAM-1, as a receptor for cell entry and do not bind VLDLR, binding to the liposome could originate only from unspecific interactions.

HRV2 Binding to VLDLR-Decorated Liposomes Is Specific. First, we incubated HRV2 with Ni^{2+} -NTA-implanted liposomes lacking receptors. CE analysis showed no shift of the liposome peak within the reproducibility of the measurements (data not shown). This result cannot fully exclude unspecific interactions because binding of the virus to the liposomes might not affect the electrophoretic mobility. However, it makes it clear that the shift of receptor-decorated liposome peak upon incubation

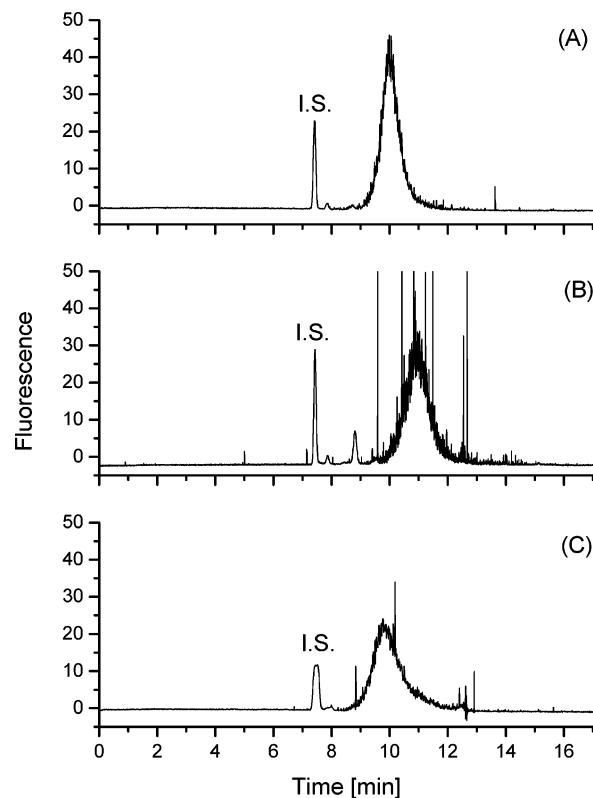


Figure 7. Electropherograms of V33333-decorated liposomes, after incubation with the minor group virus HRV2 and the major group virus HRV14, respectively. (A) V33333-decorated liposomes; (B) liposomes as in (A), after incubation with HRV2 for 1 h; (C) liposomes as in (A), after incubation with HRV14 for 1 h. I.S. fluorescein 0.7 nmol L^{-1} . PVA capillary 30.0/21.5 cm length, ID 100 μm . BGE: 50 mM Tris-HCl, pH 8.0. Incubation conditions (total incubation volume: 10 μL): (A) Ni^{2+} -NTA:V33333 = 0.7:7.4 ($\mu\text{mol L}^{-1}$); (B) V33333-decorated liposome as in (A), incubated with 0.067 $\mu\text{mol L}^{-1}$ HRV2; (C) V33333-decorated liposome as in (A), incubated with 0.061 $\mu\text{mol L}^{-1}$ HRV14.

with HRV2 (Figure 5) must be caused by the virus attaching via the receptor.

As pointed out above, in contrast to the minor group virus HRV2, major group viruses such as HRV14 do not bind members of the LDLR-family. This latter serotype was thus selected as a control. Indeed, HRV14 did not form any complex with V33333, as confirmed by CE with UV absorbance detection. When compared to the electrophoretic peaks of free V33333, free HRV14, and HRV2, the peak of HRV2 disappeared upon incubation with the receptor construct, and a peak corresponding to the V33333-virus complex was noticed. No such effect was seen for HRV14. Both virus and receptor peaks remained unchanged when the mixture of the components was analyzed (data not shown).

Thus, V33333-decorated liposomes were incubated with the respective HRV serotypes, and the incubation mixtures were analyzed by CE. All experiments were carried out with the same vesicle and receptor concentrations in the incubation solutions, and all data were acquired in one and the same series (this is relevant because it was observed that the liposomes from different preparations can possess slightly different electrophoretic properties). As expected, HRV2 shifted the liposome peak toward longer migration times (compare Figure 7A with B), and some spikes indicate the formation of virus-liposome clusters. In contrast, addition of the major group virus left the liposome peak nearly

unaffected (compare Figure 7A and C). Within the 95% confidence limit, the two peaks exhibit the same mobility (of $26.5 \times 10^{-9} \text{ m}^2 \text{ V}^{-1} \text{ s}^{-1}$, standard deviation $0.5 \times 10^{-9} \text{ m}^2 \text{ V}^{-1} \text{ s}^{-1}$, compare these data with the mobility of $24.4 \times 10^{-9} \text{ m}^2 \text{ V}^{-1} \text{ s}^{-1}$ of the HRV2-carrying liposomes in Figure 7B). This result is additional proof that the shift of the receptor-decorated liposome peak, upon addition of HRV2, does not originate from unspecific interactions, but results from the specific binding of virus to receptor-carrying liposomes.

CONCLUSIONS

CE was successfully applied to assess the specific attachment of HRV2 to receptor-decorated liposomes. Two recombinant soluble fragments of the VLDL receptor, V33333 and V123, fused to maltose binding protein and carrying a C-terminal his₆-tag, were attached to liposomes via a Ni²⁺-NTA-conjugated lipid used as a component of the liposome bilayer establishing a model of the cell membrane. The liposomes were labeled with an FL dye, dissolved in the aqueous vesicle core, thus enabling CE with LIF detection. Attachment of the virus was detected by a change of the electrophoretic mobility of the liposome, indicated by a shift of the vesicle peak. This shift was related to the biospecific interaction of the virus with the receptors. No change in the

mobility of the V33333-decorated liposomes was observed with a major group virus that uses ICAM-1 instead of members of the LDLR-family for infection. This allows the conclusion that the binding of HRV2 to these receptor-carrying liposomes is specific and represents a valid model for the attachment of the virus to the cell membrane. It also shows that a fragment of a natural receptor (V123) and an artificial receptor (V33333) behave similarly with respect to their promoting liposome binding of the virus, allowing one to extrapolate our findings to the *in vivo* situation. Further work will be conducted to analyze the next steps in virus infection that occur in the endosome such as structural changes of the virion and release of the genomic RNA.

ACKNOWLEDGMENT

This work was supported by the Austrian Science Foundation (projects P15667 and P19365). We thank Irene Goesler for the preparation of the viruses, and I. Steffan and M. Leodolter for the AAS measurements.

Received for review September 14, 2006. Accepted November 17, 2006.

AC061728M